Hindawi
Journal of Nanomaterials
Volume 2019, Article ID 5168698, 14 pages
https://doi.org/10.1155/2019/5168698

Research Article

Size-Controlled Production of Silver Nanoparticles by *Aspergillus fumigatus* BTCB10: Likely Antibacterial and Cytotoxic Effects

Asma Shahzad,[1] Hamid Saeed,[2] Mehwish Iqtedar,[1] Syed Zajif Hussain,[3] Afshan Kaleem,[1] Roheena Abdullah,[1] Saima Sharif,[4] Shagufta Naz,[4] Faiza Saleem,[1] Ayesha Aihetasham,[5] and Asma Chaudhary[6]

[1]*Department of Biotechnology, Lahore College for Women University, Lahore, Pakistan*
[2]*Section of Biomedical Sciences, University College of Pharmacy, University of the Punjab, Allama Iqbal Campus, Lahore, Pakistan*
[3]*School of Science & Engineering, Lahore University of Management Sciences (LUMS), Lahore, Pakistan*
[4]*Department of Zoology, Lahore College for Women University, Lahore, Pakistan*
[5]*Department of Zoology, University of the Punjab, Lahore, Pakistan*
[6]*University of Education, Science and Technology Section, Lahore, Pakistan*

Correspondence should be addressed to Mehwish Iqtedar; miqtedar@gmail.com

Received 30 September 2018; Revised 13 December 2018; Accepted 2 January 2019; Published 24 February 2019

Academic Editor: Jorge Pérez-Juste

The biogenesis of silver nanoparticles by fungi is an ecologically clean and nontoxic method compared to other physical and chemical methods. Thus, we aimed to discuss the mycosynthesis of extracellular size-controlled AgNPs. After comprehensive screening, *Aspergillus fumigatus* BTCB10 (KY486782) was selected for the synthesis of AgNPs of controlled size. Characterization was performed by UV-Vis spectrophotometer, Zetasizer, X-Ray Diffraction (XRD), FTIR (Fourier-transform infrared), Atomic Force Microscopy (AFM), and Scanning Electron Microscopy (SEM) along with functional assays—antibacterial and MTT assays. Data suggested that under optimized conditions, i.e., temperature 25°C, $AgNO_3$ concentration 1 mM, biomass 7 g, fungal culture age 7 days, pH 6, ratio of cell-free filtrate (CFF)/silver nitrate (3 : 2), NaCl 20%, and under dark light, the smallest size AgNPs of 0.681 nm with 100% monodispersity was obtained as evident by a zeta potential of -23.4 mV, UV-Vis band at 400 nm, and the presence of O-H and C=O groups confirmed by ATR-FTIR; XRD revealed the crystalline nature of AgNPs; additionally, cube-shaped AgNPs were revealed by Scanning Electron Microscopy (SEM). Moreover, synthesized AgNPs exhibited antibacterial activity against multidrug-resistant bacterial strains, notably, *Klebsiella pneumoniae* BTCB04, *Acinetobacter* BTCB05, *Pseudomonas aeruginosa* BTCB01, and *Escherichia coli* BTCB03, while maximum 7-fold was observed with *Acinetobacter* BTCB05. AgNPs demonstrated no cytotoxic activity against HepG2 cells; however, in combination with cisplatin, antiproliferative and cytotoxic effects became more evident and significant in comparison to control and as single agent. Taken together, the data suggested that economical and smallest size AgNPs can be biosynthesized from *Aspergillus fumigatus* BTCB10 and be used as antibacterial and antiproliferative agents in combination with current drugs against clinically relevant multiple drug-resistant bacterial and tumoral cells. Further studies are required to confirm their effects employing in vivo disease models.

1. Introduction

The synthesis of nanoparticles (one billionth part of a meter) (10^{-9}) is the most important part of nanotechnology [1]. Nanomaterials can be synthesized with various biological, chemical, and physical methods [2]. However, the production by conventional methods pose numerous challenges, such as low yield utilizing physical methods, while chemical methods are hazardous, non-eco-friendly, and extremely expensive [3]. Therefore, new ways and methods must be explored that are environment friendly, nontoxic, and inexpensive [4]. A number of known species of microorganisms (bacteria and fungi) e.g., *E. coli*, *Bacillus subtilis*, *Pseudomonas stutzeri*, *Enterobacter cloacae*, *Staphylococcus aureus*,

Fusarium oxysporum, *Agaricus bisporus*, *Penicillium citrinum*, *Trichoderma harzianum*, *Aspergillus oryzae*, *Aspergillus versicolor*, *Aspergillus terreus*, [5] unicellular and multicellular, produce efficient nanoparticles (NPs) of silver [6], titanium [7], gold [8], and platinum [9], either intracellular or extracellular [10].

Fungi have the potential to form "ecologically clean" metallic nanoparticles and are better nanofactories than plants and bacteria [11]. Numerous studies have reported that fungi are comparatively easy for large-scale nanoparticle synthesis as they produce large amounts of enzymes which assist the process [12]. Many fungal species have been investigated for the intra- or extracellular synthesis of nanoparticle such as *Fusarium oxysporum*, *Aspergillus flavus*, *Aspergillus terreus*, *Aspergillus fumigatus*, *Trichoderma viride*, *P. sajor caju*, *Pleurotus ostreatus*, *Penicillium fellutanum*, and *Macrophomina phaseolina* [13].

Previously, AgNPs of various shapes and sizes have been formed using fungi. In one such study, *Aspergillus fumigatus* produced 5 to 25 nm AgNPs with spherical shape whereas *Aspergillus terreus* also produced spherical-shaped particles with 1 to 20 nm size. Furthermore, *Fusarium oxysporum* formed 20 to 50 nm sized silver nanoparticles of spherical shape; *Trichoderma viride* formed pentagonal and hexagonal shapes with size ranging from 50 to 100 nm. Pyramid-shaped AgNPs were produced from *Phanerochaete chrysosporium* of 5 to 200 nm sizes, while from *Trichoderma asperellum* extracellular nanoparticles having nanocrystalline appearance were produced of 13 to 18 nm sizes [13, 14].

Silver nanoparticles are known for their vast applications in biomedical field (bandages, implants, and drugs/coatings), water purification, clothing, agriculture (pesticide), and most importantly antibiotics [15, 16]. Hence, they have been studied widely due to their antimicrobial activities and have also been proven efficient. One of the mechanisms suggested for the antimicrobial activity of AgNPs was that silver ions Ag^+ are discharged and get adhered to the –SH (thiol) group that is attached to the surface of the cellular membrane and disrupt its function; hence, they are responsible for their antimicrobial properties within an aqueous solution. It was reported that Ag^+ ions (free) have lower antibacterial properties in comparison to silver nanoparticles synthesized using AgCl and $AgNO_3$ [17–19].

Moreover, the cytotoxicity of silver nanoparticles was checked against different cancer cell lines including HepG2 (liver carcinoma), Caco2 (colon carcinoma), MC3T3-C1 (osteoblast) [18], MCF-7 (breast cancer), and HeLa (cervical cancer) cells [20]. Thus, we aimed to investigate the ability of *Aspergillus fumigatus* to produce silver nanoparticles using varied conditions and resources and further tested their antibacterial and antiproliferative potential using various bacterial strains and liver carcinoma cell line, HepG2, respectively.

2. Material and Methods

2.1. Reagents. Silver nitrate (Sigma-Aldrich GmbH, Germany), potassium nitrate (Riedel-de Haen, Germany), potassium di-hydrogen phosphate (Merck, USA), magnesium sulphate (Merck, USA), di-potassium hydrogen phosphate (Merck USA), ammonium sulphate (Merck, USA), yeast extract (Sigma Aldrich GmbH, Germany), and glucose (Merck, USA) were used.

2.2. Screening, Isolation, and Characterization of the Fungi. Samples were collected from industrial drain and fungi were isolated using spread plate method on potato dextrose agar (PDA), as described previously [21]. The most efficient isolate was characterized on the basis of 18S rRNA sequence analysis as described previously [22].

2.3. Extracellular Biosynthesis of Silver Nanoparticles. Silver nanoparticles were prepared as described [22]. Briefly, the procedure was divided into three phases.

2.4. Biomass Preparation and Filtration. Biomass was prepared in minimal media, pH 6, comprised of gL^{-1}: KH_2PO_4 (7.0), K_2HPO_4 (2.0), $MgSO_4{\cdot}7H_2O$ (0.1), $(NH_4)_2SO_4$ (1.0), yeast extract (0.6), and glucose (10). Media were inoculated with spores (loop full) and incubated at 25°C with continuous shaking at 120 rpm for 72 hours [23]. Biomass was filtered using Whatman filter paper (grade A) no. 1 (Ahlstrom, Spain) and was resuspended in double distilled water (100 mL) after rinsing (thrice) and later incubated at 25°C with continuous shaking (120 rpm) for 72 hours.

2.5. Extract Preparation (Cell-Free Filtrate) and Addition of Silver Nitrate Solution. The biomass was again filtered and cell-free filtrate was added to silver nitrate (1 mM) (100 mL) in equal ratio, 1 : 1. The flasks were incubated at 25°C at 120 rpm until the development of brown color indicating the formation of silver nanoparticles [23].

2.6. General Characterization of Silver Nanoparticles. Silver nanoparticles were characterized by different techniques. UV-Vis spectral analysis was performed as described previously [24]. The reduction of pure Ag ions was monitored by analyzing the UV-Vis spectrum (ORI 4000 UV-Vis spectrophotometer, Germany) within a range of A_{300} to A_{700} nm. Particle size and zeta potential of the silver nanoparticles were analyzed using Zetasizer (Malvern Nano S) (United Kingdom) as described previously [24]. For the analysis of functional groups attached with silver nanoparticles, samples were analyzed in ATR-FTIR (Bruker-OPUS) (USA). X-Ray Diffraction (XRD) (PANalytical X'Pert Powder) was used to analyze the nature of AgNPs produced. The size and shape of the silver nanoparticles were analyzed using Atomic Force Microscopy (AFM) (Park Systems) (Korea) [17] and Scanning Electron Microscopy (SEM) (Germany) was used to analyze the shape of optimized AgNPs according to previously reported method [24].

2.7. Optimization of Conditions for Synthesis of Silver Nanoparticles. AgNPs were synthesized under different physiochemical conditions to find optimum conditions favoring stable AgNPs of the smallest size range. The effect of incubation temperature on fungus growth and size of AgNPs was examined employing various temperature ranges, i.e., 25°C, 35°C, 45°C, and 55°C as reported previously [25]. The effect

of light on nanoparticle size was studied according to previous reports [10, 26, 27]. The reaction mixture was kept at both dark and light conditions to find the best condition for obtaining desired AgNPs. Also, the effect of culture age, i.e., 3-7 days, on the synthesis and size of nanoparticles was studied as reported previously [10]. According to which, *Aspergillus fumigatus* (BTCB10) (KY486782) was incubated from 3 to 7 days, and later, these culture of different age were used to inoculate media to observe its effects on the size of silver nanoparticles. The effect of pH on nanoparticle size had been reported previously [27]. Different pH that ranged from 5 to 8 was used to investigate the formation of silver nanoparticles. Silver nitrate solution of various concentrations (0.25mM, 0.5 mM, 0.75 mM, 1 mM, 2 mM, 3 mM, and 4 mM) was examined to find its effect on the formation of silver nanoparticles as described previously [28]. Another parameter studied was biomass and for that biomass of different wet weights (*w*/*v*), 1 g, 4 g, 7 g, and 10 g, was used to observe its effect on the synthesis of AgNPs as described previously [10]. A solution of 1 mM silver nitrate was added to the fungal extract (cell-free filtrate) at different ratios of 1 : 1, 1 : 2, 2 : 1, and 3 : 2 to the cell-free extract. All of these conditions were modified and applied to yield stable silver nanoparticles of small size. In addition to the abovementioned conditions, metal salts such as sodium chloride, zinc sulphate, potassium chloride, and copper nitrate were added to the cell-free filtrate to monitor the effect of these metal salts to the production and size of silver nanoparticles. The concentration studied for each metal salt was 5, 10, 15, and 20% [27].

2.8. Antibacterial Assay. The antimicrobial activity of AgNPs at various concentrations (0.1-7 μg mL^{-1}) was studied against multiple drug-resistant (MDR) bacteria by measuring zone of inhibition with some modifications according to the method [24]. The disks (Whatman filter paper) of 6 mm were loaded with AgNP concentrations 0.1, 0.5, 1, 1.5, 2, 3, 4, 5, 6, and 7 μg mL^{-1} per disk. Pathogenic strains, such as *Pseudomonas aeruginosa* BTCB01, *Staphylococcus aureus* BTCB 02, *Escherichia coli* BTCB03, *Klebsiella pneumoniae* BTCB04, and *Acinetobacter* BTCB05, were used against which antibacterial activity was checked. Fold increase for zone of inhibition was calculated to find the combined effect of both AgNPs and streptomycin (1 μg mL^{-1}) as described previously [24].

2.9. MTT Assay. The cytotoxicity of silver nanoparticles was analyzed by MTT assay. The MTT (3-(4,5-dimethylthiazol-2-yl)-2,5-diphenyltetrazolium bromide) assay was performed and modified as described previously [29]. The HepG2 cell line (human liver carcinoma cells) was obtained from Dr. Hamid Saeed, Section of Biomedical Sciences, University College of Pharmacy, University of the Punjab, Lahore, Pakistan. The HepG2 cells were cultured to analyze in vitro antiproliferative, anticancer, effects of AgNPs. The cells were cultured in 96-well plates, flat bottom, in Dulbecco's modified Eagle's medium (DMEM) containing Fetal Bovine Serum (FBS) and penicillin/streptomycin and by incubating at 37°C and 5% CO_2. The next day, the cells were treated with various concentrations (0.25 μM, 0.75 μM, and 1.50 μM) of silver nanoparticles and cisplatin for 24 hours whereas wells with media (Dulbecco's modified Eagle's medium) only served as control. Likewise, synergistic effect was analyzed by combining various concentrations of AgNPs and cisplatin in the following order: AgNPs : cisplatin (1 : 19), (1 : 3), (1 : 1), (3 : 1), and (19 : 1) and incubated for 24 hours. After 24 hours, 20 μL of MTT solution (5 mg mL^{-1}) was added and incubated for 4 hours. Thereafter, formazan crystals were solubilized in DMSO (150 μL) with slight agitation and absorbance was measured using microplate reader (595 nm).

2.10. Statistical Analysis. After optimizing the parameters, one-way ANOVA was applied to find the significance ($p \leq 0.05$) between various parameters. SPSS version 20.0 was used for the analysis.

3. Results

3.1. Molecular Characterization. BTCB10 was analyzed for molecular characterization (Figure 1(a)). Agarose gel electrophoresis revealed the presence of 597 kb band representative of *Aspergillus fumigatus* sample (Figure 1(b)). Based upon Internal Transcribed Spacer (ITS), the isolate showed 100% similarity index with *Aspergillus fumigatus* (Figure 2). The GenBank allotted the accession number KY486782 to the submitted nucleotide sequence of the isolate *Aspergillus fumigatus* BTCB10.

3.2. Optimization of Physiochemical Parameters for the Production of AgNPs. Various physicochemical parameters were utilized to find the optimum conditions for the production of AgNPs having the smallest size with selected fungus, i.e., *Aspergillus fumigatus* BTCB10 and are described below.

3.3. Temperature and Light/Dark Conditions. Dynamic light scattering (DLS) analysis demonstrated AgNPs size of 322.8 nm with 0.278 polydispersion index (PDI) at 25°C (Figure 3(a)), whereas significant ($p \leq 0.05$) increase in size was observed specified by the appearance of three peaks at 35°C with PDI 0.517, indicating polydispersity that was also confirmed by AFM results (Figure 4(a)). At 45°C, AgNPs having 414.8 nm size were obtained with PDI 0.451 (Figure 3(a)). Lastly, at 55°C, again polydispersion (two peaks) was observed with an average size of 1073.45 nm with 0.485 PDI (Figure 3(a)). Hence, AgNPs of significant ($p \leq 0.05$) small size were obtained at 25°C. In the presence of light, large-sized (750 nm) AgNPs were obtained (PDI 0.581), whereas significantly ($p \leq 0.05$) small-sized, 189.5 nm, AgNPs were formed with PDI 0.281 in the absence of light (Figure 3(b)). Therefore, the reaction in the absence of light was found optimum with size reduction of 41.29% (Figures 4(b) and 5(a)). Thus, the optimized conditions for temperature and dark are shown in Table 1 and spherical AgNPs were obtained (Figures 4(a) and 4(b)).

3.4. Fungal Culture Age and pH. Next, the effect of fungal culture age on AgNP synthesis was examined. The culture age of 3 days resulted in the production of AgNPs of 1241 nm with

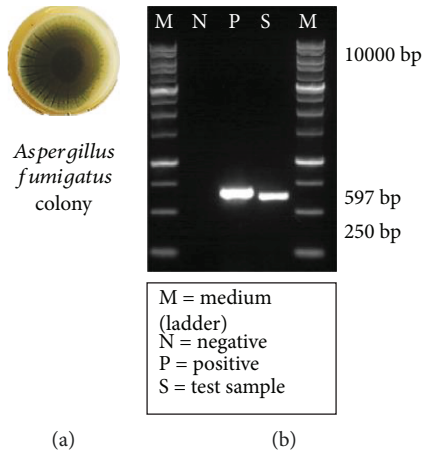

Figure 1: (a) Colony of *Aspergillus fumigatus* BTCB10 on potato dextrose agar. (b) *Aspergillus fumigatus* BTCB10 18S rDNA amplified having 597 bp.

PDI 0.463, whereas the 4th day culture produced AgNPs of 728 nm with 82.8% intensity with PDI of 0.351. The fifth and sixth day culture reduced the size to 375 nm (PDI 0.413) and 322 nm (PDI 0.437), respectively. However, the 7th day culture significantly ($p \leq 0.05$) reduced the size up to 58.17% with obtained size of 125 nm (Figures 3(c), 4(c), and 5(a)).

The effect of pH on AgNP synthesis was studied at various pH ranges. AgNP sizes of 120.98 nm and 110 nm were obtained at pH 5 (PDI 0.358) and pH 6 (PDI 0.261), respectively, whereas 157 nm size was obtained at pH 7 (PDI 0.212). Moreover, extremely large-sized AgNPs (1241 nm) (PDI 0.421) were obtained at pH 8 (Figure 3(d)). Thus, AgNPs of significant ($p \leq 0.05$) small size were obtained at pH 6—demonstrating a percentage reduction of 65.9% (Figures 3(d), 4(d), and 5(a)). Thus, the optimized conditions for culture age and pH can be seen in Table 1 and both spherical- and needle-shaped AgNPs were obtained (Figures 4(c) and 4(d)).

3.5. Substrate Concentration and Biomass Weight (Grams). The reduction in silver nitrate concentration from 0.25 mM to 1 mM resulted in significant ($p \leq 0.05$) size reduction in AgNPs from 156.2 nm to 94.75 nm with PDI ranging from 0.271 to 0.414, respectively. However, further increase in concentration from 2 to 4 mM resulted in further increase in size (Figure 3(e)). Hence, substrate concentration of 1 mM was found optimal, producing AgNP size of 94.75 nm with percentage reduction of 70.64% (Figures 4(e) and 5(a)). Different biomass weights were assessed to observe the effect on AgNP size. The biomass weight of 7 g produced the monodispersed silver nanoparticles of significant ($p \leq 0.05$) small size (94 nm), PDI of 0.312 with 70.87% percent reduction (Figures 3(f), 4(f), and 5(a)). Thus, the optimized conditions for substrate concentration and biomass weight are shown in Table 1, whereas AgNPs formed were of spherical shape (Figures 4(e) and 4(f)).

3.6. Ratio of Cell-Free Filtrate/Silver Nitrate. AgNPs of varying sizes were obtained by altering cell-free extract to silver nitrate ratio. At 2 : 1 and 1 : 1, AgNP sizes of 250.6 nm (PDI 0.411) and 128.1 nm (PDI 0.400), respectively, were obtained, whereas 1 : 2 ratio resulted in AgNP size of 99.99 nm (PDI 0.341) (Figures 3(g), 4(g), and 5(a)). Further increasing the cell-free extract to silver nitrate ratio to 3 : 2, significant ($p \leq 0.05$) reduction in AgNP size, i.e., 93.91 nm (PDI 0.218) was obtained with percentage reduction of 70.90% (Figures 3(g), 4(g), and 5(a)). Hence, the optimized conditions for CFF : $AgNO_3$ and reduction in size of AgNPs can be seen in Table 1, whereas spherical AgNPs were obtained after optimization (Figure 4(g)).

3.7. Metal Salts (w/v). Upon addition of 20% NaCl, the percentage reduction of 99.79% in size was observed producing AgNP size of 0.681 nm with PDI of 0.312 (Figures 3(h) and 5(a)) where a significant ($p \leq 0.05$) reduction was observed with reaction time of 20 seconds. Therefore, the optimized conditions for metal salts (NaCl) and reduction in size along with reaction time of AgNPs can be observed in Table 1, whereas cube-shaped AgNPs were acquired after optimization (Figure 5(a)).

3.8. Characterization of AgNPs. Characterization of optimized silver nanoparticles showed the formation of cube-shaped AgNPs which were revealed by Scanning Electron Microscopy (SEM) (Figure 5(a)). Furthermore, UV-Vis spectroscopy analysis showed Surface Plasmon Resonance (SPR) band at 400 nm (Figure 5(b)); additionally, Fourier-transform infrared (FTIR) analysis revealed the presence of OH, C=O functional groups (Figure 5(c)), size intensity (0.681%), and zeta potential of -23.4 mV (Figures 5(d) and 5(e)). XRD analysis demonstrated the crystalline nature of AgNPs (Figure 5(f)).

3.9. Functional Assays

3.9.1. Antimicrobial Assay. Different concentrations of silver nitrate ranging from 0.1 to 7 $\mu g\,mL^{-1}$ were applied against multiple drug-resistant (MDR) bacteria (Figures 6(a)–6(o)), (Table 2). In all of the cases, the zone of inhibition increased as the concentration of AgNPs increased. A 7-fold increase in the zone of inhibition was observed against *Acinetobacter* BTCB05, 3.8-fold for *Klebsiella pneumoniae* BTCB04, and 6.5-fold increase for *Pseudomonas aeruginosa* BTCB01; *Staphylococcus aureus* BTCB02 showed a 5-fold increase whereas *Escherichia coli* BTCB03 displayed 2.7-fold (Table 2). The highest zone of inhibition was observed with *Klebsiella pneumoniae* BTCB04 (33 mm) at 7 $\mu g\,mL^{-1}$ while the lowest was noted with *Pseudomonas aeruginosa* BTCB01, *Staphylococcus aureus* BTCB02, and *Acinetobacter* BTCB05 (11 mm) at 0.1 $\mu g\,mL^{-1}$ (Table 2) and their comparisons can also be studied (Figure 7(a)). Combinatorial effect (AgNPs+streptomycin 1 $\mu g\,mL^{-1}$) showed the highest zone of inhibition with *Klebsiella pneumoniae* 25 mm and the lowest was observed with *Pseudomonas aeruginosa* 11 mm (Figures 6(a)–6(o)).

3.10. MTT Assay. MTT data clearly demonstrated that AgNPs had no significant antiproliferative effects on liver carcinoma cell line (HepG2) when tested for 0.25, 0.75, and 1.50 μM concentrations (Figures 8(a)–8(c)), while significant antiproliferative effects were observed with cisplatin at increasing

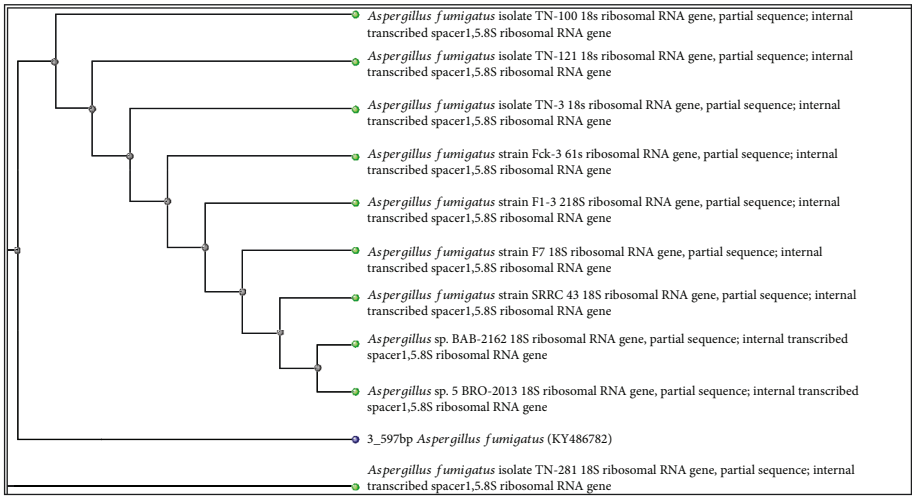

Figure 2: Phylogenetic tree identifying *Aspergillus fumigatus*.

concentration, i.e., 1.50 μM. However, when AgNPs were combined with cisplatin—for possible synergism (1 : 19), the cell viability was 44.98% which got better with increasing concentration of AgNPs and the effect became insignificant with (19 : 1) (Figure 8(c)).

4. Discussion

In the present study, *Aspergillus fumigatus* BTCB10 was used to synthesize silver nanoparticles and various physicochemical parameters were studied to find the optimum conditions for obtaining size-controlled monodispersed AgNPs. Our study demonstrated that using *Aspergillus fumigatus* BTCB10 and under optimized parameters, extracellular synthesis of AgNPs (yellow colored) was achieved within 20 seconds having 0.681 nm size with SPR band at 400 nm, whereas in a previous study, extracellular brown-colored spherical AgNPs were reported from *Aspergillus flavus*, synthesized within 72 hrs having an average size of 8.92 nm with SPR band at 420 nm [30]. Similarly, spherical silver nanoparticles (brown colored) were formed by *Aspergillus terreus* with size ranging from 1 to 20 nm, forming a SPR band at 420 nm [31]. Other *Aspergillus* species have also been investigated for the synthesis of silver nanoparticles such as *Aspergillus terreus*, *Aspergillus fumigatus*, and *Aspergillus versicolor* [13]. As compared to previous studies, the current study reported marked reduction in nanoparticle (AgNPs) synthesis time, i.e., 20 seconds, and size of AgNPs, 0.681 nm, having cube shape from *Aspergillus fumigatus* BTCB10 under optimum conditions.

4.1. Incubation Temperature. The effect of different temperatures on fungal biomass (25°C, 35°C, 45°C, and 55°C) was studied to optimize silver nanoparticle synthesis. Change in biomass weight was observed at different temperatures affecting the size of silver nanoparticles, while increased size lead to aggregation. Literature evidences support the pivotal role of temperature in various biological and chemical processes that can alter the rate of reaction. Optimum temperatures for fungi range from 25°C to 35°C; so of all the temperature ranges studied, 25°C proved optimum for growth, size (322.8 nm), and yield (11 g) of AgNPs (spherical shape) within 48 hours. Many studies have reported synthesis of silver nanoparticles with varying temperature ranges [32, 33].

4.2. Effect of Light. Numerous literature reports have already documented that dark conditions minimized the photochemical reduction of $AgNO_3$, whereas light induces cluster formation and instability in nanoparticles. Our data suggested that dark conditions facilitated (reaction time 40 hrs) size reduction of AgNPs (189.5 nm) (41.29%) with spherical shape forming a peak at 420 nm. Also, N-H, C≡C, and C-H functional groups were revealed by FTIR spectrum, which are acting as capping agents and stabilizing silver nanoparticles. In a study with *Aspergillus oryzae*, silver nanoparticles were also synthesized in the dark forming peak at 420 nm and FTIR spectrum showed presence of similar functional groups with our study, i.e., N-H vibrations and C-H stretch. Some additional functional groups were also present like C=O, C=C, C-C, and C=N [34, 35].

4.3. Age of Fungal Culture. It has been reported before that the 7-day-old culture is optimal for AgNP synthesis and favors production of nanoparticles from fungi. Similarly, we observed that 7-day-old fungal culture produced better quality AgNPs with further reduction in size to 135 nm (58.17%) forming a peak at 420 nm. FTIR spectrum revealed the presence of two functional groups N-H and C≡C. Using culture of this age, the reaction time was indeed reduced to 22 hrs and produced needle-shaped AgNPs as evidenced by Atomic Force Microscopy (AFM). The favorable effects of culture age could be explained by enhanced enzyme production affecting AgNP size. In a study, silver nanoparticles were produced from *Fusarium oxysporum* of 7-day-old culture that proved optimum. Young culture showed better results than older culture having the same incubation time. However, the study showed extended reaction time of 48 hours as compared to the current study where it was 22 hrs for forming peak at 413 nm. AgNPs formed by *Fusarium*

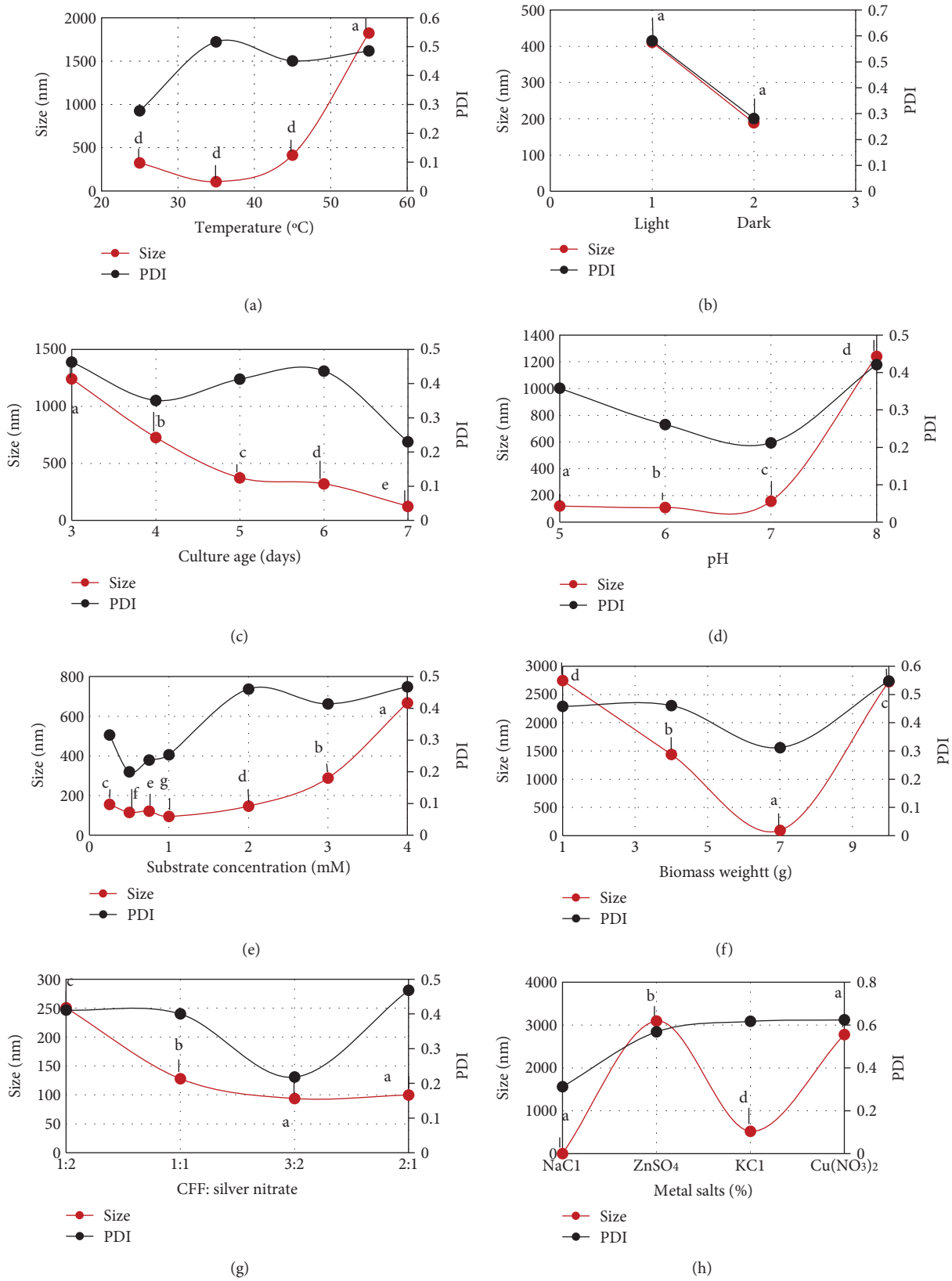

Figure 3: Mycosynthesis of silver nanoparticles under various physicochemical conditions. (a) Temperature (°C). (b) Dark/light conditions. (c) Culture age (days). (d) pH. (e) Substrate concentration. (f) Biomass weight. (g) Ratio CFF/$AgNO_3$. (h) Metal salts.

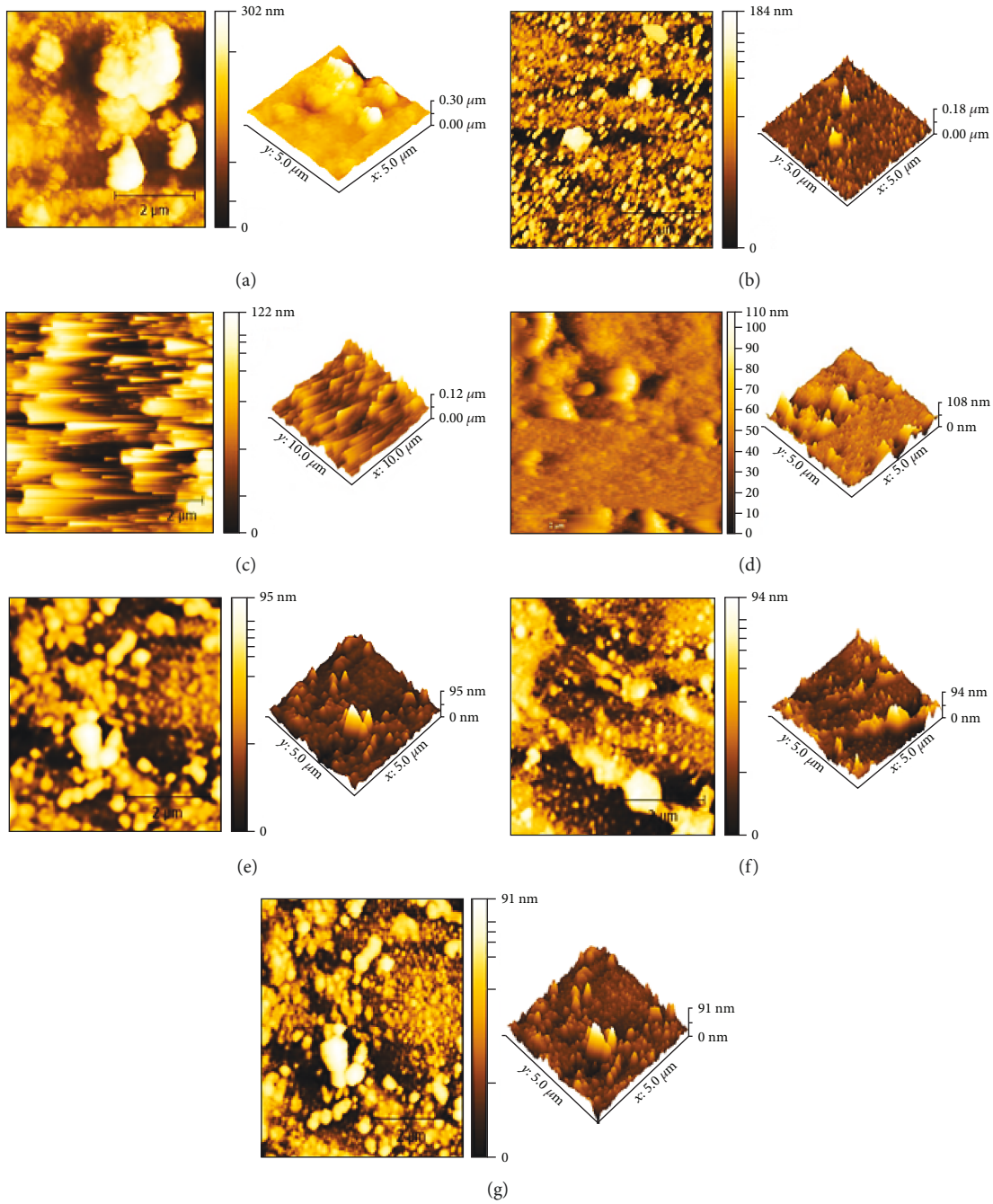

Figure 4: Atomic Force Microscopic (AFM) analysis of mycosynthesized AgNPs under different optimum physicochemical conditions (a) Temperature. (b) Dark conditions. (c) Culture age. (d) pH. (e) Substrate concentration. (f) Biomass weight. (g) Ratio CFF/$AgNO_3$.

oxysporum showed presence of amide, cysteine, and carboxyl functional groups [10].

4.4. pH. Previous work reported that nanoparticles were stable at pH 6 and are attributed to optimum working conditions for Nicotinamide Adenine Dinucleotide Hydrogen (NADH) between pH 6.5 and 7 which plays an important role in microbial production of AgNPs [36]. In the present study, the effect of various pH ranges (5–8) on AgNP synthesis and size revealed that pH 6 was the optimal condition that reduced the size to 110 nm with 65.9% size reduction in 12 hours. At this pH, reaction time was also reduced from 22 hr to 12 hr. Atomic Force Microscopy (AFM) showed the formation of spherical AgNPs forming excitation peak at 410 nm whereas the presence of O-H, C≡C, and N-H functional groups were detected by FTIR analysis. However, aggregation occurred as the pH shifted towards more acidic conditions; similarly, in one of the study, AgNPs were synthesized through *Penicillium fellutanum* at various pH (5 to 7) where pH 6 was found optimum with a reaction time of 24 hours [27]. In another study with *Fusarium oxysporum*, reduced size of silver nanoparticles was achieved

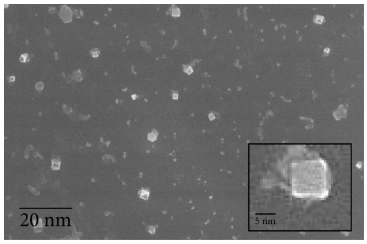

(a)

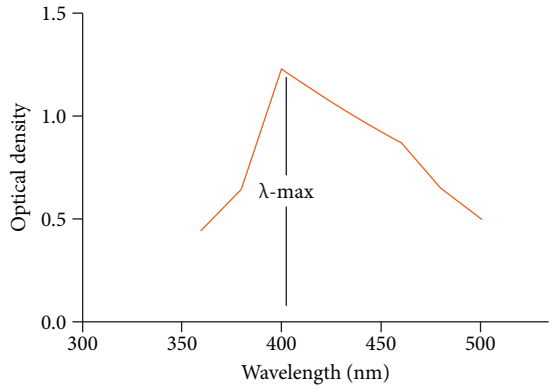

(b)

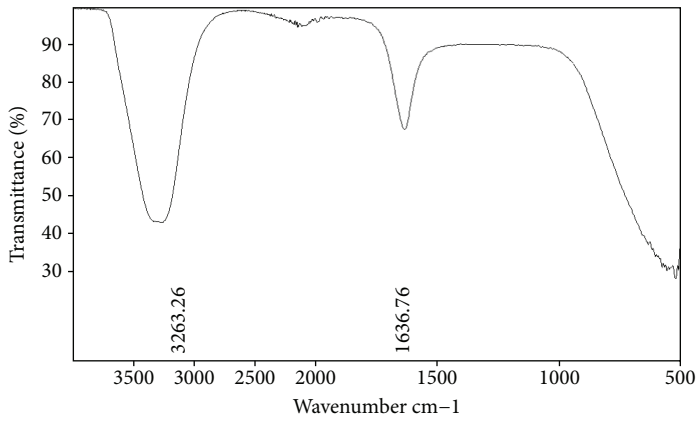

(c)

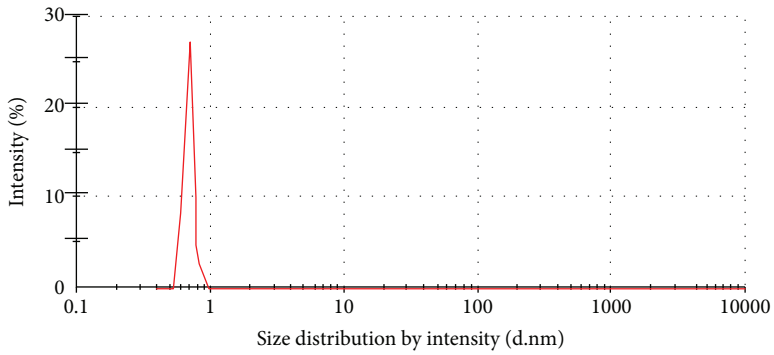

(d)

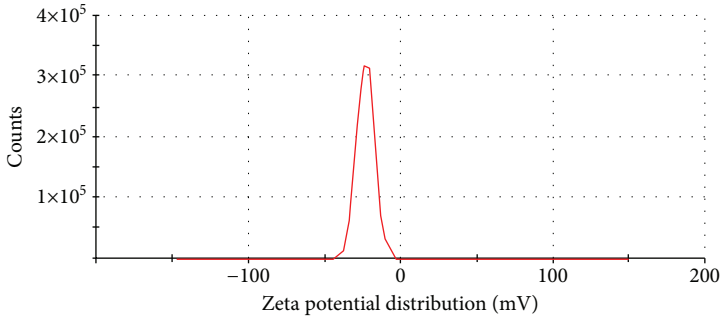

(e)

Figure 5: Continued.

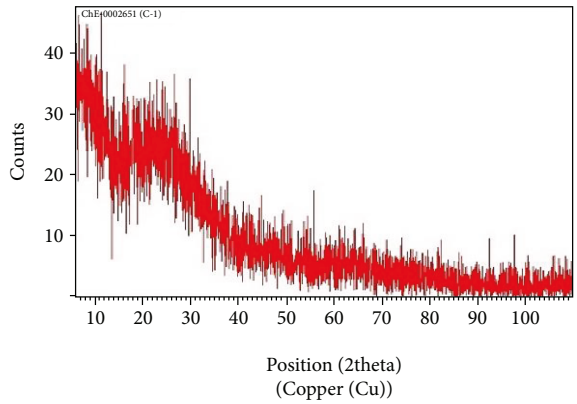

(f)

Figure 5: Characterization of silver nanoparticles formed under optimum conditions (NaCl 20%). (a) SEM analysis showing cube-shaped AgNPs. (b) UV-Vis spectroscopic analysis. (c) Fourier-transform infrared (FTIR) analysis. (d) Zetasizer analysis. (e) Zeta potential of AgNPs. (f) XRD analysis.

Table 1: AgNP synthesis by *Aspergillus fumigatus* BTCB10 under optimum physiochemical conditions.

Sr. no.	Parameters	Optimized conditions	Incubation time (hrs)	AgNP size (nm)	Shape of AgNPs	PDI	Reduction in size (%)
1	Temperature	25°C	48	322.8	Spherical	0.278	—
2	Light/dark	Dark	40	189.5	Spherical	0.281	49.29
3	Culture age	7 days	22	125	Needle	0.437	58.17
4	pH	6	12	110	Spherical	0.261	65.9
5	Substrate conc.	1 mM	4	94	Spherical	0.254	70.64
6	Biomass weight	7 g	3	94	Spherical	0.312	70.87
7	CFF : silver nitrate	3 : 2	2	93.94	Spherical	0.218	70.90
8	Metal salts (NaCl)	20%	20 seconds	0.681	Cube	0.312	99.97

at pH 6 but with reaction time of 72 hrs and absorbance peak at 420 nm which is closer to ours while revealing cysteine, amide, and carboxyl groups as stabilizing agents [10].

4.5. Substrate Concentration. Further effect of substrate concentration (silver nitrate mM) on AgNP synthesis was observed which showed that with an increase in substrate concentration, the size and aggregation of nanoparticles also increased. In a study with *Penicillium polonicum*, different concentrations (0.5, 1, 2, and 3 mM) of silver nitrate were applied to check its effect on silver nanoparticles where 1 mM concentration proved optimum with sharp peak (430 nm) whereas shift of the peaks was observed at 0.5, 2, and 3 mM concentrations in 24 hrs. The presence of O-H, C=O, C=C, and N-H groups was also detected in their study [37]. However, among all the concentrations analyzed in the present study, 1 mM proved optimum in producing 94.75 nm size AgNPs obtaining peak at 422 nm at 4 hours of reaction time. The presence of functional groups (capping agents) in cell-free extract (O-H, C=O) caused reduction in the size of AgNPs to 70.65%. As the concentration of silver nitrate (substrate) increased, the competition between silver ions and functional groups led to large-sized nanoparticles along with instability and aggregation.

4.6. Biomass. As per the literature evidences, increased biomass is associated with increased enzyme productivity that might be responsible for the formation of silver nanoparticles. In one such study, various biomass weights (5, 10, 15, and 20 g) were used to analyze the effect on silver nanoparticle size and synthesis by *P. polonicum*. The optimized wet weight was 10 g establishing a peak at 430 nm. The presence of O-H, C=O, C=C, and N-H groups was detected in their study [37]. In comparison, the present study revealed that the optimum biomass weight for silver nanoparticle synthesis was 7 g which reduced the size to 94 nm with 70.87% reduction in size. The shape revealed by AFM was spherical forming excitation peak at 414 nm. FTIR spectrum also showed the involvement of N-H, C≡C, and O-H groups in the stabilization of nanoparticles. Increased biomass not only reduced the size of AgNPs but also reduced the reaction time to 3 hrs that might be due to the presence of excessive amount of enzymes. However, with further increase in biomass, the AgNP size increased, which might be attributed to saturated cellular environment.

4.7. Ratio of Cell-Free Filtrate/Silver Nitrate Solution. Among all the ratios studied for cell-free filtrate/silver nitrate (CFF), 3 : 2 (v/v) was effective in reducing the size of spherical

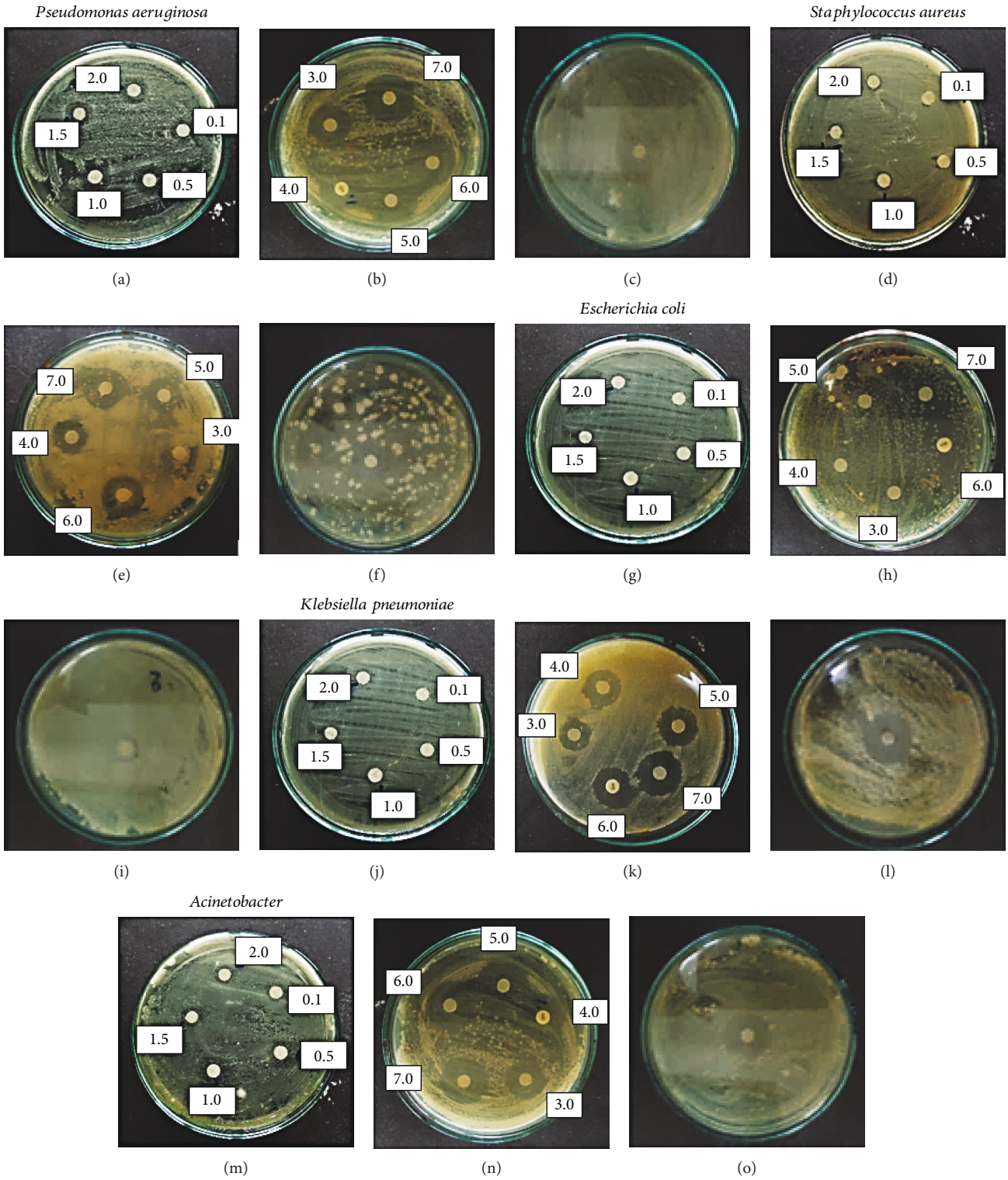

Figure 6: Antimicrobial activity of AgNPs at various concentrations against multiple drug-resistant bacteria. (a, b) *Pseudomonas aeruginosa* (AgNPs 0.1-7 μg mL^{-1}). (c) Combined effect of AgNPs (1 μg mL^{-1}) and streptomycin (1 μg mL^{-1}) against *Pseudomonas aeruginosa*. (d, e) *Staphylococcus aureus* (0.1-7 μg mL^{-1}). (f) Combined effect of AgNPs (1 μg mL^{-1}) and streptomycin (1 μg mL^{-1}) against *Staphylococcus aureus*. (g, h) *Escherichia coli* (0.1-7 μg mL^{-1}). (i) Combined effect of AgNPs (1 μg mL^{-1}) and streptomycin (1 μg mL^{-1}) against *Escherichia coli*. (j, k) *Klebsiella pneumoniae* (0.1-7 μg mL^{-1}). (l) Combined effect of AgNPs (1 μg mL^{-1}) and streptomycin (1 μg mL^{-1}) against *Klebsiella pneumoniae*. (m, n) *Acinetobacter* (0.1-7 μg mL^{-1}). (o) Combined effect of AgNPs (1 μg mL^{-1}) and streptomycin (1 μg mL^{-1}) against *Acinetobacter*.

Table 2: Antimicrobial activity of AgNPs against multiple drug-resistant bacterial isolates.

MDR strains	Zone of inhibition (mm) AgNP concentrations (μg mL^{-1})										Fold increase	Combinatorial effect (AgNPs+streptomycin) (mm)
	0.1	0.5	1	1.5	2	3	4	5	6	7		
Pseudomonas aeruginosa BTCB01	11	12	19	20	21	22	24	25	27	30	6.5	11
Staphylococcus aureus BTCB02	11	13	14	15	16	22	24	25	25	27	5.0	22
Escherichia coli BTCB03	13	14	15	17	14	18	18.5	21	22	25	2.7	24
Klebsiella pneumoniae BTCB04	15	16	18	19	25	27	29	30	32	33	3.8	25
Acinetobacter BTCB05	11	18	20	21	22	25	26	28	29	31	7	23

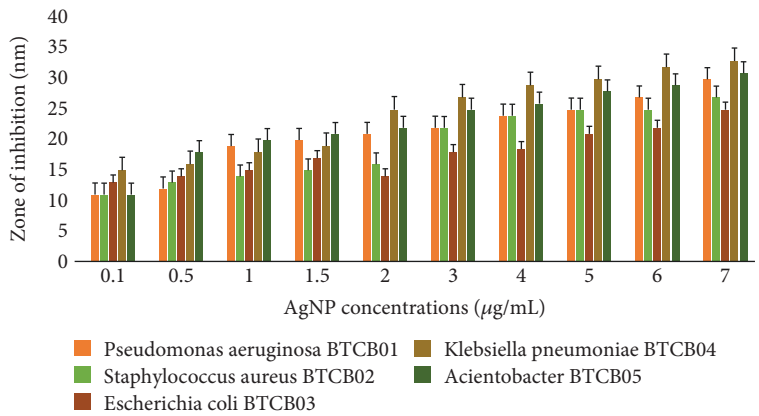

Figure 7: Antibacterial activity against MDR AgNPs at various concentrations (0.1-7 μg mL^{-1}) against multiple drug-resistant bacteria (BTCB01 to BTCB05).

AgNPs to 93.91 nm with 70.9% size reduction with a reaction time of 2 hrs. Excitation peak obtained was at 424 nm with the presence of N-H, C≡C, and O-H functional groups. It was also observed that increased CFF volume led to a decrease in silver nanoparticle size. Similar findings have been reported previously, suggesting that increased CFF volume resulted in increased production of enzymes that might lead to the formation of small-sized nanoparticles. Similarly, in one of the study with *P. polonicum*, various $AgNO_3$: CFF ratios (5 : 5, 6 : 4, 7 : 3, 8 : 2, and 9 : 1) were applied for the synthesis of silver nanoparticles; among those, 8 : 2 proved optimum for AgNP synthesis. An absorption peak was observed at 430 nm which is closer to our study and reaction time recorded was 60 minutes. Spherical-shaped AgNPs were reported in their study along with O-H, C=O, C=C, and N-H functional groups [37]. In a similar study, AgNP synthesis was mediated with *P. glomerata* where varying quantities of cell-free filtrate from 0.1 to 1.9 mL were used. According to which, high cell-free filtrate, i.e., 1.9 mL, facilitated AgNP synthesis having an absorption peak at 420 nm [38].

4.8. Metal Salts. The effect of NaCl has been studied previously on size and stability of AgNPs [27]. Therefore, metal salts were added to the cell-free filtrate to monitor their effect on silver nanoparticle formation. The cell-free filtrate with sodium chloride turned yellow within 20 seconds and produced AgNPs of 0.681 nm size with cube shape. Moreover, no further change in color was observed indicating stability of AgNPs also confirmed by UV-Vis peak at 400 nm and zeta potential of -23.4 mV, explainable by significant boost in Raman signal and further corroboration by X-ray diffractogram showing intense peaks of 2θ position (Cu) at 38°, 44.5°, 64.7°, and 77.5°. FTIR revealed the presence of N-H and C≡C functional groups. In a previous study, silver nanoparticles were synthesized by *Penicillium fellutanum* and the effect of different NaCl concentrations (0.1 to 0.5%) was observed on AgNP synthesis. The optimum concentration identified was 0.3% NaCl with particles ranging from 5 to 25 nm having a reaction time of 24 hours [27]. However, in the current study, at higher concentration of about 20% NaCl, AgNP synthesis was rapid with a reaction time of 20 seconds and the size obtained was 0.681 nm confirmed by Zetasizer as compared to the previous study.

4.9. Effect of AgNPs against Multiple Drug-Resistant (MDR) Bacteria. It has been reported previously that the silver nanoparticles synthesized by fungus *Candida albicans* showed antibacterial activity against *Staphylococcus aureus* and *Escherichia coli* producing 21 mm and 17 mm zones of inhibition, respectively [39]. Antibacterial activities of AgNPs synthesized by *Aspergillus oryzae* were studied with 4 kinds of strains, namely, *Staphylococcus aureus*, *Escherichia coli*, *Klebsiella pneumoniae*, and *Bacillus subtilis*. Silver nanoparticles (7.22 nm) with concentration 15 μg mL^{-1} formed zone of inhibition with *Staphylococcus aureus* (8 mm), *Escherichia*

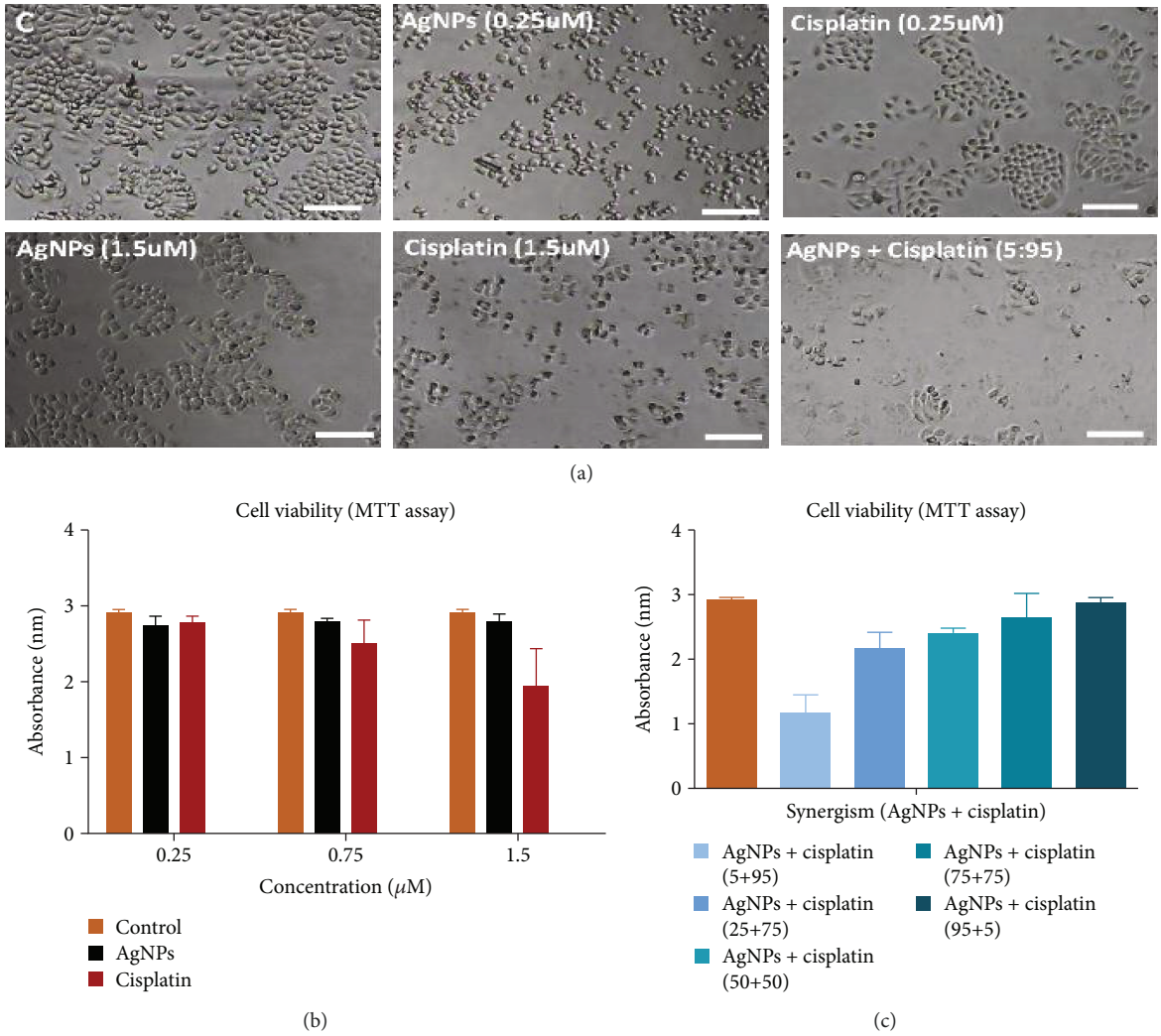

Figure 8: Cytotoxic assay. (a) HepG2 cancer cells at different experimental conditions. (b) Cytotoxic effect of AgNPs, cisplatin against HepG2 cancer cells. (c) Synergistic effect of AgNPs and cisplatin against HepG2 cells.

coli (15 mm), *Klebsiella pneumoniae* (19 mm), and *Bacillus subtilis* (13 mm) [34]. Combinatorial effect (AgNPs+streptomycin) (1 μg mL^{-1}) showed the highest zone of inhibition with *Klebsiella pneumoniae* 25 mm and the lowest zone was observed with *Pseudomonas aeruginosa* at 11 mm. Moreover, *Staphylococcus aureus* showed 22 mm and *Acinetobacter* revealed 23 mm. In a similar study with silver nanoparticles, *Klebsiella pneumoniae* showed 8 mm and *Staphylococcus aureus* showed 12 mm zone of inhibition with 50 μg mL^{-1} [24] whereas in our study greater effect was observed at small concentration of 1 μg mL^{-1} with both of the strains.

In our study, antimicrobial activity was performed against multiple drug-resistant (MDR) strains with AgNPs (0.1 to 7 μg mL^{-1}). Among all strains, *Klebsiella pneumoniae* BTCB04 exhibited maximum zone of inhibition of 33 mm at AgNP concentration of 7 μg mL^{-1}. In comparison to the previous study, the zone of inhibition was greater at lower concentration (7 μg mL^{-1}); moreover, AgNP size was also small (0.6 nm) as compared to the previous study (7.22 nm). Thus, it was revealed that smaller-sized silver nanoparticles displayed enhanced antibacterial activity due to their large surface area and it can further associate itself with more capping agents/functional groups. Similarly, antibacterial activity with AgNPs was also observed in another study where AgNPs of 7.22 nm size with concentration 15 μg mL^{-1} presented maximum zone of inhibition against *Bacillus subtilis* (16 mm), *E. coli* (15 mm), and *Staphylococcus aureus* (15 mm) and the highest fold increase (0.66) was recorded with *Staphylococcus aureus* [39].

4.10. Effects of AgNPs, Alone or in Combination, against Liver Carcinoma Cell Line (HepG2). The results suggested that biosynthesized AgNPs had no toxic effects against liver carcinoma cell lines (HepG2). Likewise, another study further confirmed nontoxic potential of silver nanoparticles against HepG2 cells (<0.5 mg L^{-1}), rather it was found to enhance cell proliferation [29]. Another study with *Phanerochaete chrysosporium* showed no toxicity towards cancer cells (fibroblast) at a concentration of 12.5 μg/mL; however, various concentrations of 1.5 μg/mL-200 μg/mL were also tested [40]. Similar to the abovementioned findings, our data suggested that in all tested concentrations, AgNPs did not

exhibit any cytotoxic effects on HepG2 cell lines. Contrary to our findings, AgNPs obtained from *Streptomyces rochei* MHM13 exhibited enhanced cytotoxic effects against HepG2 cell lines [41]. Another study with *Aspergillus niger* with HT-29 (colon cancer) showed toxicity right after 72 hrs with cell survival of only 13% at 160 g/mL [42].

These differences could be explained by differences in AgNP source and concentration of AgNPs used. However, combining AgNPs with cisplatin resulted in significant synergism in the form of cytotoxicity. In a study with *Aspergillus similanensis*, cytotoxic activity was not found below 1.17 μM against HepG2 cell lines [43]. In our results, even at lower concentration of 0.75 μM, cell viability (%) was 107; furthermore, even after increasing the concentration to 1.50 μM, there was still no cytotoxic activity (cell viability; 107%), therefore reporting no toxicity to HepG2 cells.

5. Conclusion

In conclusion, our data suggested that *Aspergillus fumigatus* BTCB10 under optimal conditions, temperature 25°C, silver nitrate concentration 1 mM, biomass 7 g, fungal culture age 7 days, pH 6, ratio of CFF/silver nitrate (3 : 2), and NaCl 20% under dark could be utilized for economical production of AgNPs with the smallest size. Moreover, to our knowledge, this is the first study to report cube-shaped AgNPs, synthesized from *Aspergillus fumigatus* BTCB10 using the above-mentioned parameters, of the smallest size (0.681 nm) with minimum reaction time—possessing antibacterial effects against medically important resistant bacterial strains along with negligible antiproliferative effects on cancer cell line. Nevertheless, AgNPs in combination with anticancer drugs (cisplatin) exhibited positive response.

Data Availability

All the data are presented in the manuscript; however, any additional data not mentioned in the manuscript if required will be made available.

Conflicts of Interest

The authors declare that there is no conflict of interest regarding the publication of this paper.

Acknowledgments

The authors acknowledge the Higher Education Commission, Pakistan, for providing funds under Access to Scientific Instruments Program. The authors also acknowledge the Central Laboratory Facility of Lahore College for Women University, Lahore, Pakistan, for giving access to high-tech equipment.

References

[1] K. AbdelRahim, S. Y. Mahmoud, A. M. Ali, K. S. Almaary, A. E. Z. M. A. Mustafa, and S. M. Husseiny, "Extracellular biosynthesis of silver nanoparticles using *Rhizopus stolonifer*," *Saudi Journal of Biological Sciences*, vol. 24, no. 1, pp. 208–216, 2017.

[2] N. Durán, M. Durán, M. B. de Jesus, A. B. Seabra, W. J. Fávaro, and G. Nakazato, "Silver nanoparticles: a new view on mechanistic aspects on antimicrobial activity," *Nanomedicine: Nanotechnology, Biology and Medicine*, vol. 12, no. 3, pp. 789–799, 2016.

[3] S. M. El-Sonbaty, "Fungus-mediated synthesis of silver nanoparticles and evaluation of antitumor activity," *Cancer Nanotechnology*, vol. 4, no. 4-5, pp. 73–79, 2013.

[4] V. Rathod and E. Ranganath, "Synthesis of monodispersed silver nanoparticles by Rhizopus stolonifer and its antibacterial activity against MDR strains of Pseudomonas aeruginosa from burnt patients," *International Journal of Environmental Sciences*, vol. 1, no. 7, pp. 1582–1592, 2011.

[5] A. Ahmad, S. Senapati, M. I. Khan et al., "Intracellular synthesis of gold nanoparticles by a novel alkalotolerant actinomycete, *Rhodococcus* species," *Nanotechnology*, vol. 14, no. 7, pp. 824–828, 2003.

[6] P. Azmath, S. Baker, D. Rakshith, and S. Satish, "Mycosynthesis of silver nanoparticles bearing antibacterial activity," *Saudi Pharmaceutical Journal*, vol. 24, no. 2, pp. 140–146, 2016.

[7] E. Babaei, A. Dehnad, N. Hajizadeh, H. Valizadeh, and S. F. S. Reihani, "A study on inhibitory effects of titanium dioxide nanoparticles and its photocatalytic type on Staphylococcus aureus, Escherichia coli and Aspergillus flavus," *Applied Food Biotechnology*, vol. 3, no. 2, pp. 115–123, 2016.

[8] M. Fayaz, C. S. Tiwary, P. T. Kalaichelvan, and R. Venkatesan, "Blue orange light emission from biogenic synthesized silver nanoparticles using *Trichoderma viride*," *Colloids and Surfaces B: Biointerfaces*, vol. 75, no. 1, pp. 175–178, 2010.

[9] M. D. Balakumaran, R. Ramachandran, P. Balashanmugam, D. J. Mukeshkumar, and P. T. Kalaichelvan, "Mycosynthesis of silver and gold nanoparticles: optimization, characterization and antimicrobial activity against human pathogens," *Microbiological Research*, vol. 182, pp. 8–20, 2016.

[10] S. M. Husseiny, T. A. Salah, and H. A. Anter, "Biosynthesis of size controlled silver nanoparticles by *Fusarium oxysporum*, their antibacterial and antitumor activities," *Beni-Suef University Journal of Basic and Applied Sciences*, vol. 4, no. 3, pp. 225–231, 2015.

[11] K. Kawata, M. Osawa, and S. Okabe, "In vitro toxicity of silver nanoparticles at noncytotoxic doses to HepG2 human hepatoma cells," *Environmental Science and Technology*, vol. 43, no. 15, pp. 6046–6051, 2009.

[12] N. T. Khan and S. U. A. Rehman, "Synthesis of AgNPs using *Aspergillus terreus* and evaluation of its antimicrobial activity," *Advanced Techniques in Biology & Medicine*, vol. 4, no. 4, p. 190, 2016.

[13] K. S. Siddiqi, A. Husen, and R. A. K. Rao, "A review on biosynthesis of silver nanoparticles and their biocidal properties," *Journal of Nanbiotechnology*, vol. 16, no. 1, p. 14, 2018.

[14] J. K. Patra and K. H. Baek, "Green nanobiotechnology: factors affecting synthesis and characterization techniques," *Journal of Nanomaterials*, vol. 2014, Article ID 417305, 12 pages, 2014.

[15] M. Eltarahony, S. Zaki, and D. Abd-el-Haleem, "Concurrent synthesis of zero- and one-dimensional, spherical, rod-, needle-, and wire-shaped CuO nanoparticles by *Proteus mirabilis* 10B," *Journal of Nanomaterials*, vol. 2018, Article ID 1849616, 14 pages, 2018.

[16] S. M. Ali, N. M. H. Yousef, and N. A. Nafady, "Application of biosynthesized silver nanoparticles for the control of land snail *Eobania vermiculata* and some plant pathogenic fungi,"

Journal of Nanomaterials, vol. 2015, Article ID 218904, 10 pages, 2015.

[17] A. U. Khan, N. Malik, M. Khan, M. H. Cho, and M. M. Khan, "Fungi-assisted silver nanoparticle synthesis and their applications," *Bioprocess and Biosystems Engineering*, vol. 41, no. 1, pp. 1–20, 2018.

[18] C. S. Danna, D. G. S. M. Cavalcante, A. S. Gomes et al., "Silver nanoparticles embedded in natural rubber films: synthesis, characterization, and evaluation of *in vitro* toxicity," *Journal of Nanomaterials*, vol. 2016, Article ID 2368630, 10 pages, 2016.

[19] M. Murphy, K. Ting, X. Zhang, C. Soo, and Z. Zheng, "Current development of silver nanoparticle preparation, investigation, and application in the field of medicine," *Journal of Nanomaterials*, vol. 2015, Article ID 696918, 12 pages, 2015.

[20] L. Salazar, M. J. Vallejo López, M. Grijalva, L. Castillo, and A. Maldonado, "Biological effect of organically coated *Grias neuberthii* and *Persea americana* silver nanoparticles on HeLa and MCF-7 cancer cell lines," *Journal of Nanomaterials*, vol. 2018, Article ID 9689131, 11 pages, 2018.

[21] W. F. Harrigan, *Laboratory Methods in Food Microbiology*, Elsevier, New York, 1998.

[22] S. M. Karst, M. S. Dueholm, S. J. McIlroy, R. H. Kirkegaard, P. H. Nielsen, and M. Albertsen, "Retrieval of a million high-quality, full-length microbial 16S and 18S rRNA gene sequences without primer bias," *Nature Biotechnology*, vol. 36, no. 2, pp. 190–195, 2018.

[23] Z. Sadowski, I. H. Maliszewska, B. Grochowalska, I. Polowczyk, and T. Koźlecki, "Synthesis of silver nanoparticles using microorganisms," *Materials Science-Poland*, vol. 26, no. 2, pp. 419–424, 2008.

[24] K. Jyoti, M. Baunthiyal, and A. Singh, "Characterization of silver nanoparticles synthesized using *Urtica dioica* Linn. leaves and their synergistic effects with antibiotics," *Journal of Radiation Research and Applied Sciences*, vol. 9, no. 3, pp. 217–227, 2016.

[25] V. Vijay Kalaskar, N. Kasinatha, V. Mallikarjuna Subrahmanyam, and J. Venkata Rao, "Optimization of extracellular acid protease production from Aspergillus niger by factorial design," *Journal of Microbiology, Biotechnology and Food Sciences*, vol. 4, no. 2, pp. 132–136, 2014.

[26] L. Ma, W. Su, J. X. Liu et al., "Optimization for extracellular biosynthesis of silver nanoparticles by *Penicillium aculeatum* Su1 and their antimicrobial activity and cytotoxic effect compared with silver ions," *Materials Science and Engineering: C*, vol. 77, pp. 963–971, 2017.

[27] K. Kathiresan, S. Manivannan, M. A. Nabeel, and B. Dhivya, "Studies on silver nanoparticles synthesized by a marine fungus, *Penicillium fellutanum* isolated from coastal mangrove sediment," *Colloids and Surfaces B: Biointerfaces*, vol. 71, no. 1, pp. 133–137, 2009.

[28] H. Korbekandi, Z. Ashari, S. Iravani, and S. Abbasi, "Optimization of biological synthesis of silver nanoparticles using *Fusarium oxysporum*," *Iranian Journal of Pharmaceutical Research : IJPR*, vol. 12, no. 3, pp. 289–298, 2013.

[29] S. J. Yu, J. B. Chao, J. Sun, Y. G. Yin, J. F. Liu, and G. B. Jiang, "Quantification of the uptake of silver nanoparticles and ions to HepG2 cells," *Environmental Science & Technology*, vol. 47, no. 7, pp. 3268–3274, 2013.

[30] P. Velusamy, G. V. Kumar, V. Jeyanthi, J. Das, and R. Pachaiappan, "Bio-inspired green nanoparticles: synthesis, mechanism, and antibacterial application," *Toxicology Research*, vol. 32, no. 2, pp. 95–102, 2016.

[31] T. M. Abdelghany, A. M. H. al-Rajhi, M. A. al Abboud et al., "Recent advances in green synthesis of silver nanoparticles and their applications: about future directions. A review," *Bio-NanoScience*, vol. 8, no. 1, pp. 5–16, 2018.

[32] V. Sarsar, M. K. Selwal, and K. K. Selwal, "Biogenic synthesis, optimisation and antibacterial efficacy of extracellular silver nanoparticles using novel fungal isolate Aspergillus fumigatus MA," *IET Nanobiotechnology*, vol. 10, no. 4, pp. 215–221, 2016.

[33] C. Krishnaraj, R. Ramachandran, K. Mohan, and P. T. Kalaichelvan, "Optimization for rapid synthesis of silver nanoparticles and its effect on phytopathogenic fungi," *Spectrochimica Acta Part A: Molecular and Biomolecular Spectroscopy*, vol. 93, pp. 95–99, 2012.

[34] P. Phanjom and G. Ahmed, "Effect of different physicochemical conditions on the synthesis of silver nanoparticles using fungal cell filtrate of *Aspergillus oryzae* (MTCC no. 1846) and their antibacterial effect," *Advances in Natural Sciences: Nanoscience and Nanotechnology*, vol. 8, no. 4, article 045016, 2017.

[35] M. Kumari, S. Pandey, V. P. Giri et al., "Tailoring shape and size of biogenic silver nanoparticles to enhance antimicrobial efficacy against MDR bacteria," *Microbial Pathogenesis*, vol. 105, pp. 346–355, 2017.

[36] Z. M. Xiu, Q. B. Zhang, H. L. Puppala, V. L. Colvin, and P. J. J. Alvarez, "Negligible particle-specific antibacterial activity of silver nanoparticles," *Nano Letters*, vol. 12, no. 8, pp. 4271–4275, 2012.

[37] S. Neethu, S. J. Midhun, E. K. Radhakrishnan, and M. Jyothis, "Green synthesized silver nanoparticles by marine endophytic fungus Penicillium polonicum and its antibacterial efficacy against biofilm forming, multidrug-resistant Acinetobacter baumanii," *Microbial Pathogenesis*, vol. 116, pp. 263–272, 2018.

[38] A. Gade, S. Gaikwad, N. Duran, and M. Rai, "Green synthesis of silver nanoparticles by Phoma glomerata," *Micron*, vol. 59, pp. 52–59, 2014.

[39] G. Rahimi, F. Alizadeh, and A. Khodavandi, "Mycosynthesis of silver nanoparticles from *Candida albicans* and its antibacterial activity against *Escherichia coli* and *Staphylococcus aureus*," *Tropical Journal of Pharmaceutical Research*, vol. 15, no. 2, pp. 371–375, 2016.

[40] M. Saravanan, S. Arokiyaraj, T. Lakshmi, and A. Pugazhendhi, "Synthesis of silver nanoparticles from Phenerochaete chrysosporium (MTCC-787) and their antibacterial activity against human pathogenic bacteria," *Microbial Pathogenesis*, vol. 117, pp. 68–72, 2018.

[41] H. Abd-Elnaby, G. Abo-Elala, U. Abdel-Raouf, A. Abd-elwahab, and M. Hamed, "Antibacterial and anticancer activity of marine *Streptomyces parvus*: optimization and application," *Biotechnology & Biotechnological Equipment*, vol. 30, no. 1, pp. 180–191, 2016.

[42] W. Chengzheng, W. Jiazhi, C. Shuangjiang et al., "Biogenic synthesis, characterization and evaluation of silver nanoparticles from *Aspergillus niger* JX556221 against human colon cancer cell line HT-29," *Journal of Nanoscience and Nanotechnology*, vol. 18, no. 5, pp. 3673–3681, 2018.

[43] A. A. Ramos, M. Prata-Sena, B. Castro-Carvalho et al., "Potential of four marine-derived fungi extracts as anti-proliferative and cell death-inducing agents in seven human cancer cell lines," *Asian Pacific Journal of Tropical Medicine*, vol. 8, no. 10, pp. 798–806, 2015.